# **Supercritical Fluid Nanospray Mass Spectrometry**

Mahmoud Elhusseiny Mostafa<sup>1</sup>, James P. Grinias<sup>2</sup>, and James L. Edwards<sup>1</sup>\*

<sup>1</sup>Department of Chemistry and Biochemistry, Saint Louis University, 3501 Laclede Ave, St Louis, MO 63103, USA.

ABSTRACT: Supercritical fluids are typically electrosprayed using an organic solvent makeup flow to facilitate continuous electrical connection and enhancement of electrospray stability. This results in sample dilution, loss in sensitivity, and potential phase separation. Pre-mixing the supercritical fluid with organic solvent has shown substantial benefits to electrospray efficiency and increased analyte charge state. Presented here is a nanospray mass spectrometry system for supercritical fluids (nSF-MS). This split flow system used small i.d. capillaries, heated interface, inline frit, and sub-micron emitter tips to electrospray quaternary alkyl amines solvated in supercritical CO<sub>2</sub> with a 10 % methanol modifier. Analyte signal response was evaluated as a function of total system flow rate (0.5 – 1.5 mL/min) that is split to nanospray a supercritical fluid with linear flow rates between 0.07-0.42 cm/sec, and pressure ranges (15 – 25 MPa). The nSF system showed mass-sensitive detection based on increased signal intensity for increasing capillary i.d. and analyte injection volume. These effects indicate efficient solvent evaporation for the analysis of quaternary amines. Carrier additives generally decreased signal intensity. Comparison of the nSF-MS system to the conventional SF make-up flow ESI showed 10-fold signal intensity enhancement across all the capillary i.d.s. The nSF-MS system likely achieves rapid solvent evaporation of the SF at the emitter point. The developed system combined the benefits of the nano emitters, sCO<sub>2</sub>, and the low modifier percentage which gave rise to enhancement in MS detection sensitivity.

#### Introduction

High-efficiency electrospray is critical to achieving the full potential of mass spectrometry (MS) systems. Reduction of emitter tip i.d. to low micron and submicron dimensions for nanospray improves ionization efficiency and signal response.<sup>1</sup> The tip size of the emitter defines the initial droplet size and solvent evaporation.<sup>2-6</sup> One method to enhance evaporation is the use of high volatility solvents. Supercritical fluids (SFs) can function as a solvent for electrospraying. 7 It operates at elevated temperature and pressure but undergoes phase conversion at room temperature and atmospheric pressure. The supercritical fluid carbon dioxide (sCO<sub>2</sub> at >7.3 MPa and >31.1 °C) has been used to enhance solvent evaporation and ionization efficiency.<sup>8</sup> It uses organic modifiers like methanol to improve ionization efficiency and additives like formic acid to improve chromatographic performance.9-11 Previous work on the fundamental characterization of the SFs showed a  $10^6 - 10^9$  enhancement in evaporation of sCO<sub>2</sub> compared to organic solvents.<sup>12</sup> This results in higher detection sensitivity compared to organic solvents. 13, 14

Pioneering work by the Olesik group showed enhanced ESI detection sensitivity and increased the analyte charge state when  $10-40\,\%\,$  sCO<sub>2</sub> was added to the organic spray solvent. At these high organic solvent levels, the state is considered enhanced-fluidity liquid chromatography (EFLC) rather than a supercritical fluid state. <sup>15</sup> This provided increased diffusivity, lower viscosity, faster analysis, and higher detection sensitivity over a wide variety of analytes. <sup>16-18</sup>

Conventional SF chromatography (SFC) systems coupled to MS often use a post-column organic solvent make-up flow to achieve stable ESI. 11, 19-24 This organic make-up flow avoids analyte precipitation but ultimately results in sample dilution. 14, 25 If the solvent ratio is not optimized, the supercritical fluid will phase separate into both a gas and liquid residue resulting in

subsequent loss of signal.<sup>26</sup> Sub-critical temperature and pressure SFC increased sensitivity compared to LC for polyaromatic standards.<sup>27</sup> Theoretical modeling indicated that supercritical conditions provide smaller droplets and shorter droplet lifetimes allowing for faster evaporation compared to the subcritical conditions.<sup>28</sup>

Based on the success of previous SF-MS work, a capillary nanospray supercritical fluid (nSF) system is presented to achieve nanoflow rates.<sup>29</sup> The use of 90% sCO<sub>2</sub> enhances solvent evaporation upon exiting the emitter tip, diminishes solvent effects, and increases signal response compared to full bore makeup flow SF.<sup>19, 30, 31</sup> Quaternary amines were analyzed to evaluate the desolvation process in nSF-MS. Low levels of organic solvent modifiers in sCO<sub>2</sub> result in higher MS signal response.<sup>32</sup> This nSF coupling uses small i.d. emitters, embedded photopolymerized frit, and heated connections to achieve a 10-fold enhanced signal.

## Materials and Methods Reagents and capillaries.

Twenty-five, fifty, and seventy-five µm i.d. (360 µm outer diameter) fused silica capillary tubes were purchased from Polymicro Technologies (Phoenix, AZ). A zero dead volume (ZDV) IDEX High-Pressure PEEK union was purchased from Cole Parmer (Vernon Hills, IL). Fiberglass heater tapes were purchased from Omega Engineering (Norwalk, CT). A digital display PID temperature controller thermostat was purchased from Twidec (Suzhou, China). A 300 mm "Hot Pocket" column heater, LC-MS grade water, Optima LC-MS grade methanol, formic acid, hydrofluoric acid, and ammonium acetate were all purchased from Thermo Fisher Scientific (Pittsburgh, PA). Hexanal, octanal, decanal, sodium bicarbonate, and sodium cyanoborohydride were purchased from MilliporeSigma (Saint Louis, MO). 4-trimethyl amino butylamine (TMBA) was synthesized in-house for tagging aldehydes.<sup>33</sup>

#### Capillary interface.

<sup>&</sup>lt;sup>2</sup>Department of Chemistry and Biochemistry, Rowan University, 201 Mullica Hill Rd., Glassboro, NJ 08028, USA.

<sup>\*</sup> Corresponding author email: jim.edwards@slu.edu

Capillary nanotip orifices were fabricated using a trap-end frit, laser-pulled method. When the sum of the polyimide coating. Photopolymerized frits were generated using a monomer mix of 350  $\mu L$  trimethylolpropane trimethacry-late and 150  $\mu L$  of glycidyl methacrylate with 7.9 mg of benzoin methyl ether (BME). The porogenic solvent was prepared by mixing 250  $\mu L$  toluene and 750  $\mu L$  isooctane. The monomer solution (300 mL) was added to the porogen solution and sonicated for 15 minutes. The frit mixture is loaded into the capillary and polymerization was initiated with UV-lamp (UVP, Cambridge, UK): wavelength was 365 nm, 6 watts, 0.12 amps, time for the reaction was 30 minutes at ambient temperature.

Nanospray tips were generated using a laser fiber puller model P-2000 (Sutter Instruments, Novato, CA, USA) with heating time 420 msec, velocity 80 msec, delay time 150 msec, pulling time 225 msec. The nano emitter fritted capillary was etched in hydrofluoric acid (51 %) to open the fine tip resulting in the nanospray emitter. The 25, 50, and 75  $\mu m$  i.d. capillaries were trimmed to 2 cm. The capillary before the split was wrapped in a heating tape to maintain the temperature of the SF. The short emitter, inline photopolymerized frit, and the proximate position to the MS achieved nanospray (Figure 1). 250  $\mu m$  i.d. x 6.27 cm, 500  $\mu m$  i.d. x 3.16 cm, and 1000  $\mu m$  i.d. x 20.2 cm splitters where used for the 25, 50, and the 75  $\mu m$  i.d. emitters respectively.

#### Sample preparation: Reductive amination of aldehydes.

1 mM hexanal, octanal, and decanal standard solutions were prepared in 1.5 mL methanol. 500 mM sodium bicarbonate buffer in water (pH 7.5) was prepared in a separate vial. A reductive amination tagging reaction was performed using a 500 mM sodium cyanoborohydride (NaBH<sub>3</sub>CN) reducing agent in methanol. <sup>35</sup> 50 mM TMBA was prepared in methanol media. 120  $\mu$ L of the tag was added to the aldehydes followed by a 7.2  $\mu$ L buffer then vortexing for 1 minute. 12  $\mu$ L of the reducing agent was then added followed by another 1-minute vortexing where fizzing would be seen in the reaction vial. This provides 6:1 buffer: aldehyde and 3.6: 1 reducing agent: aldehyde. The mixture was then stored at 5 °C for 5 hours to complete the reaction. The sample was dried at room temperature in a vacuum centrifuge. Reconstitution in 1.5 mL methanol yielded a 1 mM tagged aldehydes stock mixture (**Figure 2A**). All samples were analyzed at 50  $\mu$ M.

#### Supercritical fluid system.

The Shimadzu 'Nexara UC' supercritical fluid system (Columbia, MD) is driven by a modifier pumping (LC-30A) and CO<sub>2</sub> solvent delivery unit LC-30ADSF system. The CO<sub>2</sub> gas delivery unit has a built-in pump head cooler and uses a micro-volume double plunger pump. The system contains a communication bus module (CBM-20A) and (SIL-30AC) autosampler. The temperature was controlled by (CTO-20AC) heating oven and the pressure controlled by an SFC-30A back pressure regulator (BPR). The system premixes the sCO<sub>2</sub> with the modifier prior to the sample injection point.

## Mass Spectrometer.

Experiments were performed on an LTQ XL Linear Ion Trap mass spectrometer (Thermo Fisher Scientific, San Jose, CA). A Thermo nanospray Flex<sup>TM</sup> ion source emitter in positive ionization mode was used for the characterization of the nanospray at 1 - 4 kV spray voltage, 150 °C capillary temperature. A Thermo source ESI housing heated probe (HESI) was used for the full flow sample introduction. The optimized parameters were as follows: sheath gas was 10, auxiliary gas was 7, sweep gas was 5, and spray voltage was 3 kV. The capillary temperature was 275 °C. The mass range was from 50 - 300 m/z, scan time was 1 micro-scan, maximum injection time 10 msec, AGC was 1E6.

Data Processing: XCalibur, GraphPad Prism, and RStudio.

Data files in (.RAW) format were displayed on Thermo Xcalibur Qual browser software from Thermo Scientific. Graphing was done using GraphPad Prism9 software (San Diego, CA). The 3D heat maps of signal intensities as a function of pressure and linear velocity were displayed using RayShader. It is an open-sourced 3D mapping package for programming and displaying data using RStudio platform.<sup>36</sup>

#### Results and discussion.

#### Coupling strategy.

A SF-nanospray-MS system was designed and implemented to achieve a signal response higher than the conventional nanospray systems. It provides higher solvent evaporation with smaller droplets and more volatile solvents. This system uses a heated, post-BPR split flow with a photopolymerized frit in the nanoemitter (Figure 1). To achieve a nanospray of the SF effluent, 25, 50, and 75 μm i.d. post-split capillaries with a 500 nm – 2 μm laser-pulled emitter tip were used. The split flow allows higher volumetric flow rates (1.1 mL/min) through the SF pump, which are necessary to achieve the appropriate backpressure for sCO<sub>2</sub>. A splitless flow nanospray SF system was attempted but the backpressure was unstable at low pre-split volumetric flow rates while higher flow rates yielded rupture of the frit/tip. The distance from the emitter tip to the MS interface and the analyte conductivity also affect the electrospray droplet size.<sup>37</sup> The distance between the emitter and the MS orifice was optimized at 4 mm for this system.<sup>6</sup> 90 % sCO<sub>2</sub> with 9.9 % methanol and 0.1 % formic acid was used for comparing the nSF-MS signal across different emitter i.d.s. This is to normalize for the ionic conductivity of the ionizing media.

The small i.d. capillary, photopolymerized frit, and pulled tip were all necessary to maintain nanospray, stable pressure, and consistent spray. The absence of any one of these resulted in bubble formation as reported elsewhere.<sup>25</sup>

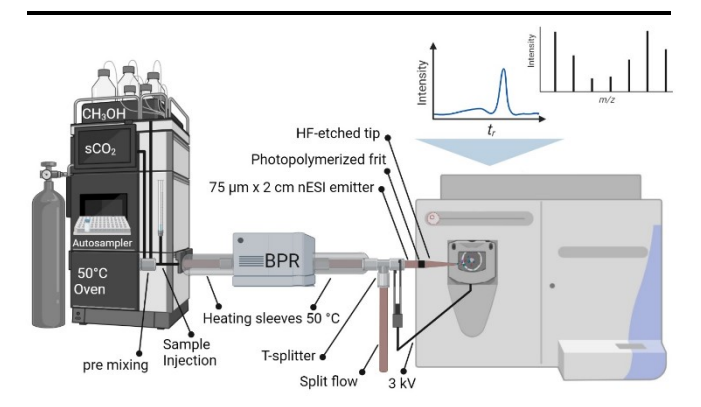


Figure 1: nSF-MS supercritical fluid-nanospray-MS split-flow coupling strategy. A diagram of the supercritical fluid coupled to the mass spectrometer (nSF-MS) using a post-back pressure regulator (BPR) split flow and an inline embedded photopolymerized nano emitter.

A nanoemitter without the frit resulted in unstable outlet pressure readings and unstable spray during the injection sequence. A 0.5 cm frit was used across all nanoemitter to achieve consistent nanospray. While the frit adds only a small component to the pressure drop, experimentally we found it critical to maintaining a stable spray.

The operating pressure, temperature, and flow rates necessary to maintain the signal were investigated.  $^{38}$ ,  $^{39}$  Using a flow injection analysis configuration, signal response from the nanospray was evaluated as a function of flow rate, pressure, and solvent composition. The pre-split SF volumetric flowrate of  $500-1500~\mu L/min$  was split to 35 - 96~nL/min using the  $25~\mu m$  i.d., 95 - 261~nL/min using the  $50~\mu m$  i.d., and 192 - 528~nL/min using the  $75~\mu m$  i.d. emitter. The calculated linear velocity was done according to the Hagen-Poiseuille equation.  $^{40}$  The linear flow rate ranges were 0.15-0.42~cm/sec for the  $25~\mu m$ , 0.14-0.40~cm/sec for the  $50~\mu m$ , and 0.07-0.21~cm/sec for the  $75~\mu m$  i.d. nano emitters. A higher split ratio did not provide a reproducible MS signal whereas lower ratios resulted in phase collapsing as indicated by unstable spray and bubbles formation (data not shown), limiting the maximum linear velocity with the  $75~\mu m$  i.d. nano emitters.

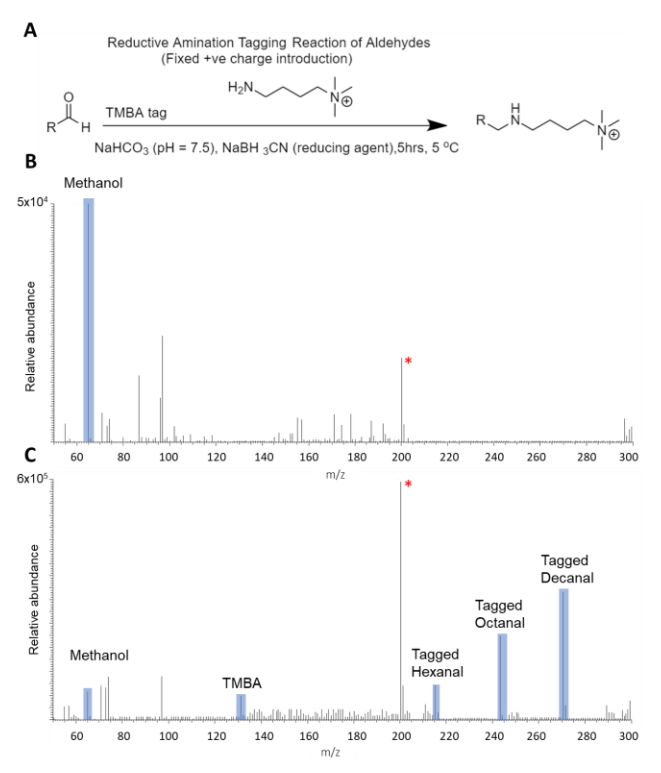


Figure 2: Nanospray-supercritical fluid-MS of tagged aldehydes. A) The reductive amination coupling reaction scheme for tagging aldehydes. B) Mass spectrum of the background signal. C) Mass spectrum of the injected plug. \* background contaminant

The nSF system temperature was maintained using heated connections at 50 °C. The absence of this heater resulted in a substantially diminished signal. The system showed inconsistent nanospray from 30 – 40 °C and irreproducible low signal intensity from 40 – 45 °C. A constant temperature of 50 °C was achieved using a post-BPR heater that wraps around the system up to the split tee. While no heater was applied after the split, temperature of the nanospray chamber was found to be near 50 °C, likely due to residual heat transfer. The back pressure was set to 15 – 25 MPa at 50 °C and the carrier was 90:10 sCO2:methanol to prevent phase collapse before reaching the emitter tip critical to achieving spray. Methanol adsorption and density gradient profile were absent in the low pressure nSF-MS system. We have the substantial profile were absent in the low pressure nSF-MS system.

To evaluate the electrospray process, we focused on desolvation by selecting molecules that remove consideration of the proton transfer step. To ensure that the developed system is capable of proton transfer, nanospraying myoglobin was performed using the developed nSF-MS system (**Supplemental Figure 1**). A comparable signal response was found compared to nanospraying 100 %

methanol. In order to characterize for the desolvation without proton affinity consideration, alkyl aldehydes standards were derivatized with a fixed charge tag as the analytes. 43, 44 Tagging of hexanal, octanal, and decanal was done with a TMBA tag as shown in **Figure 2A**. **Figure 2B** shows the background MS spectrum from a blank injection with a base peak of the methanol dimer. 45 The MS spectrum of the TMBA tag and the tagged aldehydes in **Figure 2C** shows the appearance tagged analyte from the SF nanospray system. The longer acyl chains showed higher signal intensity across all parameters investigated. This may be due to different interactions between analytes and the ionizing modifiers affecting the ionization mechanism and the corresponding MS detection sensitivity. 46, 47

#### nSF optimization.

The robustness of the system was evaluated by comparing analyte signal intensity and the nESI current to changes in linear flow rate, spray voltage, and solvent composition. Nanospraying 10% CH<sub>3</sub>OH in sCO<sub>2</sub> using a 75 µm i.d. nESI emitter at 50 °C and a linear velocity range from 0.07 – 0.21 cm/sec showed a maximum nESI current of 0.66 μA (Figure 3A). The tagged aldehydes increased in signal intensity as a function of linear velocity from 0.07 to 0.14 cm/sec. The signal intensity trends plateau from 0.14 to 0.17 cm/sec. A decreasing signal intensity trend was obtained by flowing faster than 0.17 cm/sec. Flowing slower than 0.07 cm/sec gave low (1E2) to no signal response. Irreproducible and distorted signals were found spraying faster than 0.21 cm/sec. The maximum signal response from varying the linear velocity was found at 0.14 cm/sec sCO<sub>2</sub> at 18 MPa. This point was chosen to optimize the voltage using the MS signal response to nSF spraying the tagged aldehydes (Figure 3B). Signal increased by increasing voltage up to +3 kV followed by a signal drop. Applying voltage lower than +1.5 kV showed condensed liquid bubbles at the nESI tip and lost signal. The optimum operational voltage for the nSF-MS system was +3.0 kV. nESI current increased with the voltage from 0 -2 kV followed by a shallowing from 2-4 kV.

The methanol percentage in sCO<sub>2</sub> determines the physical condition of the carrier mixture. 48 Figure 3C shows the change in tagged aldehydes signal response as the percentage of methanol increased. Less than 5 % of methanol gave no detectable MS signal whereas 5-8 % gave inconsistent electrospray. The spray inconsistencies in the low percent methanol are likely due to the low dielectric constant of the medium and failure to properly conduct the voltage to the distal tip. The tagged aldehydes signal stabilized from 9 % methanol and plateaued at 10 %. nESI current increased with the % methanol but the tagged aldehydes signal intensity was level between 10 – 30 % methanol. 10 % methanol was chosen for the optimization and characterization of the nSF-MS system to maximize desolvation. Stable nanospray was indicated by  $0.6 - 0.9 \,\mu\text{A}$  nESI current. This was acquired by flowing faster than 0.24, 0.22, and 0.10 cm/sec for the 25, 50, and 75 µm i.d. emitter respectively, voltage > 1.5 kV, and premixing more than 9 % methanol in sCO<sub>2</sub>.

The density of the supercritical fluid is controlled by the modifier percentage and the operating pressure. <sup>49</sup> **Supplemental Figure S-2** shows the mobile phase pump pressure change as a function of methanol percentage at different nSF operational flow rates (550 – 1500  $\mu$ L/min sCO<sub>2</sub>). A linear correlation is shown between the inlet mobile phase pump pressure and the methanol percentage from 0 – 40 %. An exponentially increasing trend was found from 40 – 66 % methanol, depending on the flow rate. Beyond that, the nSF-MS system was not able to maintain the supercritical fluid state and the system density error stopped the pump.

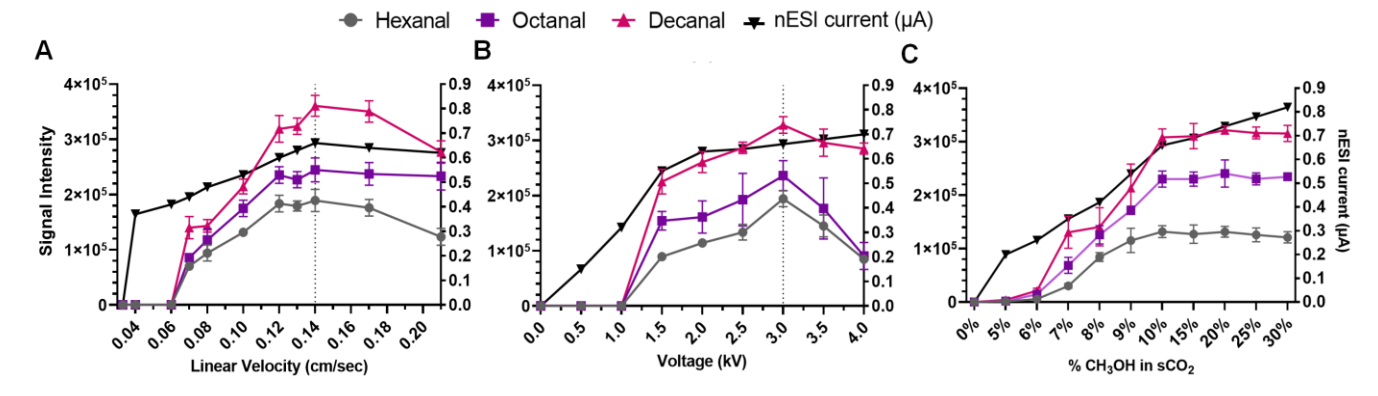


Figure 3: Optimization of nanospray-supercritical fluid-MS (nSF-MS). Optimization of the A) linear velocity B) voltage C) % CH3OH modifier using the signal intensities of the tagged aldehydes nanosprayed by 75  $\mu$ m i.d. nESI emitter at 18 MPa, 50 °C on the nSF-MS system (n=3, error bars are standard deviation).

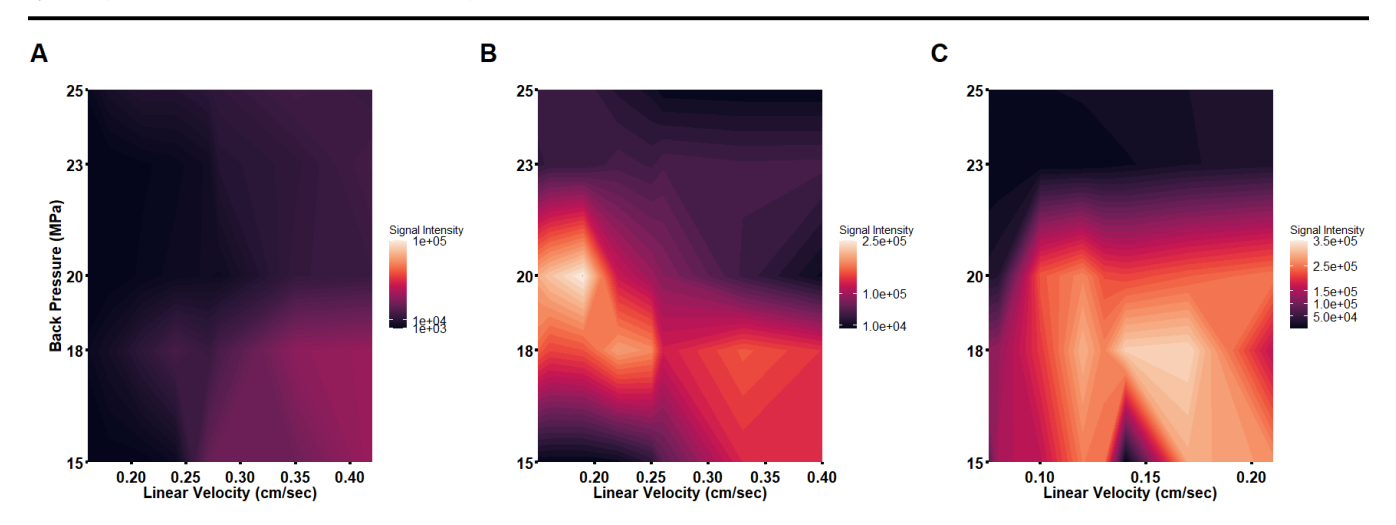


Figure 4: Optimization of nanospray-supercritical fluid-MS (nSF-MS) signal response of quaternary amine-tagged octanal using different i.d.s nanoemitters. 3D heat maps signal intensity (average of n=3) of the tagged octanal as a function of pressure (15-25 MPa) and linear velocity using A) 25  $\mu$ m (0.15 – 0.42 cm/sec), B) 50  $\mu$ m (0.14 – 0.40 cm/sec), and C) 75  $\mu$ m i.d. (0.07 – 0.21 cm/sec) nano emitter interfaces.

Increasing the percentage of methanol increased the pump pressure exerted to maintain the SF required pressure.  $^{50}$  The nSF system showed a reproducible MS signal response using 10-50~% methanol in sCO<sub>2</sub> without phase separation. Based on the Hagen-Pouiselle equation and the pump pressure as a function of solvent composition, the viscosity of the carrier stream elevates dramatically beyond 50~% methanol, consistent with a loss of the supercritical fluid state.

Examination of the emitter i.d. effect on the nSF-MS signal as a function of backpressure (15 – 25 MPa) and linear velocity was done using 25, 50, and 75  $\mu$ m i.d. interfaces. 3D heatmaps of averaged signal intensities are shown in **Figure 4** and **Supplemental Figure S3-S5**. The effects from pressure, velocity, and tip diameter are discussed below.

For nSF-MS operation pressure: Early studies found that 10 % methanol has a critical pressure above 13.17 MPa $^{48,\,51}$  This may explain the low signal intensity operating below 15 MPa using 10 % methanol in sCO2. Increasing the pressure from 15 to 18 MPa showed a significant signal intensity increase. Maintaining the BPR lower than 15 MPa of the tagged octanal showed a very low signal intensity. A comparable signal response was found from 18 - 20 MPa whereas signal intensity drops when pressure increases from 20 - 25 MPa. This might be attributed to the dramatic variation of signal response at elevated SF pressure.  $^{52}$  BPR above 25

MPa required a mobile phase pumping pressure exceeding the limits of the pump.

For the linear velocity: The ranges were 0.15-0.42 cm/sec for the  $25~\mu m$ , 0.14-0.40 cm/sec for the  $50~\mu m$  i.d. , and 0.07-0.21 cm/sec for the  $75~\mu m$  i.d. Flowing faster than 0.42 cm/sec for the  $25~\mu m$  i.d., 0.40 cm/sec for the  $50~\mu m$  i.d., and 0.21 cm/sec for the  $75~\mu m$  i.d. emitters showed a significant signal intensity drop whereas slower than 0.15~cm/sec for the  $25~\mu m$  i.d., 0.14~cm/sec for the  $50~\mu m$  i.d., and 0.07~cm/sec for the  $75~\mu m$  i.d. resulted in complete loss of signal. The optimum operating pressure was 18~MPa giving the highest nSF-MS signal across different velocities.

The increased pressure in the open tube SF results in differences in mass flow at a fixed linear velocity in a fixed restrictor. This may explain the small change in signal response with pressure increase using the 25  $\mu m$  i.d. emitter (Supplemental Figure S3). The observed signal intensity drops in the nSF-MS system using 50  $\mu m$  i.d. nESI emitter were found when flowing faster than 0.33 cm/sec (Supplemental Figure 4). The optimized linear velocities of the 25, 50, 75  $\mu m$  i.d. emitters were (0.28, 0.26, and 0.14 cm/sec) respectively. The highest signal intensities of the tagged aldehydes were found at 0.14 cm/sec using the 75  $\mu m$  i.d. ESI interface. Increasing i.d. the capillary was followed by a signal intensity increase (Figure 5A). This is due to more mass injected as the

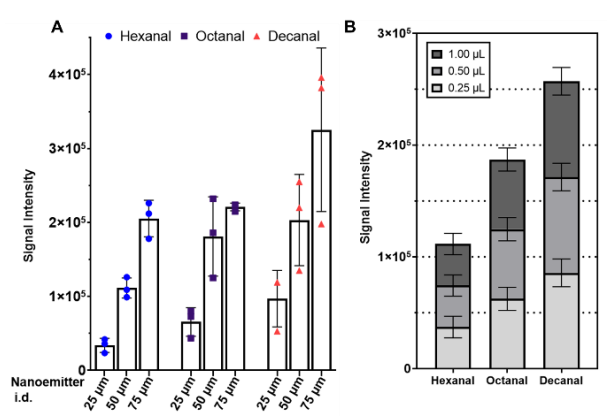
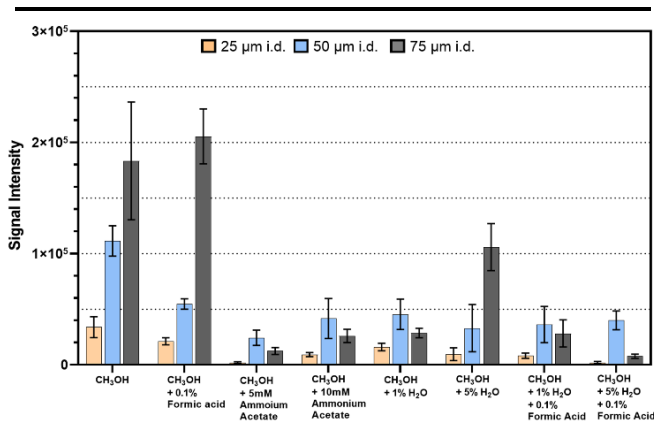


Figure 5: Nanospray-supercritical fluid-MS mass-sensitive detection. The nSF-MS signal (n=3, error bars are standard deviation) of tagged aldehydes as a function of A) Nanoemitter i.d. and B) Injection volumes using a 75  $\mu$ m i.d. interface at 18MPa, 50°C, and 0.14cm/sec.



**Figure 6: Modifier additives effect on supercritical fluid nanospray.** Nanospray-supercritical fluid-MS (nSF-MS) signal response (n=3, error bars are standard deviation) using different modifier additives in 25, 50, and 75 μm i.d. emitter.

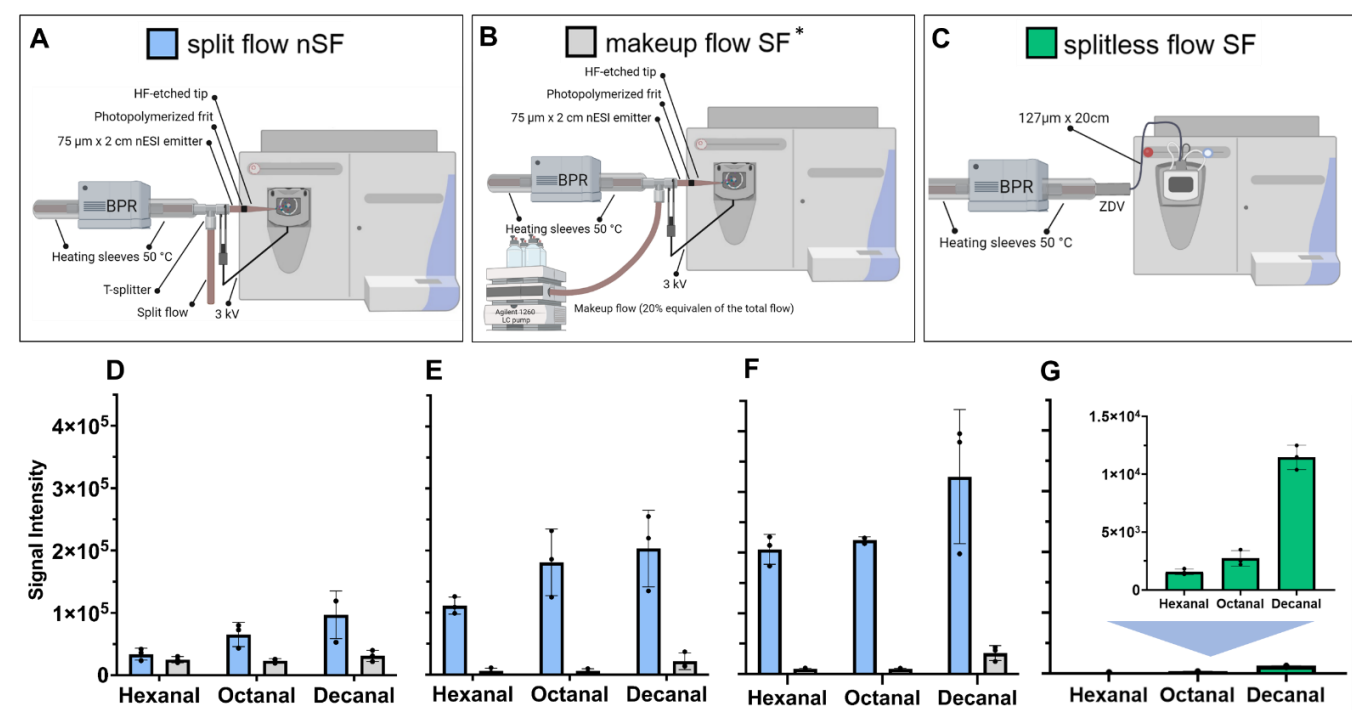


Figure 7: Comparison of different coupling strategies using the tagged aldehydes signal. Supercritical fluid-mass spectrometer coupling by A) split flow nSF (blue), B) makeup flow SF (grey), and C) splitless flow SF (green). Comparison of tagged aldehydes signal using a split flow versus makeup flow of 1:0.1 mL/min sCO<sub>2</sub>:CH<sub>3</sub>OH (0.1 % formic acid) using D) 25  $\mu$ m, E) 50  $\mu$ m, and F) 75 $\mu$ m photopolymerized inline embedded frit. \* the make up flow was 0.2 mL/min CH<sub>3</sub>OH (0.1 % formic acid). G) 100  $\mu$ m HESI interface. (n=3, error bars are standard deviation)

capillary i.d. increased.  $^{53}$  Injection of 1  $\mu L$  sample on the split-flow resulted in 58, 158, 320 nL mass injected on the 25, 50, and the 75  $\mu m$  i.d. emitters respectively. The mass injected from the 75  $\mu m$  i.d. emitter was 2 times more than the 50  $\mu m$  i.d. emitter and 5 times that on the 25  $\mu m$  i.d. emitter.

Detector signal response from nanospray can be either mass sensitive or concentration-sensitive depending on the flow rate and ionization efficiency.  $^{54}$  Injections of 0.25, 0.5, and 1.00  $\mu L$  at 18 MPa, 0.14 cm/sec, 50 °C was done using the 75  $\mu m$  i.d. emitter. Figure 5B shows mass-sensitive detector response of the nSF system. Increasing the injection volume showed an increase in the percentage of relative abundance of the tagged aldehydes in the MS spectrum using the same 75  $\mu m$  i.d. emitter (Supplemental Figure

S-6). Overall, mass sensitive response was supported by: increasing the mass injected by altering the split ratios with increasing i.d. (Figure 5A); increasing mass injected on the same i.d. emitter (Supplemental Figure 6), and increasing the capillary i.d. showed a percentage relative abundance increase (Figure 5B). Reproducible MS signal response was found with varying emitter i.d. and injection volume. The mass-sensitive detection indicates a high level of ionization efficiency.

# Supercritical carrier effect.

Supercritical fluid chromatography (SFC) typically uses additives like formic acid or ammonium acetate which act as ionization enhancers.<sup>11</sup> Water has been also used to increase polarity and improve peak shape.<sup>55</sup> Clustering of alkali metal ions with methanol

is a major contributor to signal suppression in SF-MS. <sup>56</sup> **Figure 6** shows the effect of modifiers on the supercritical fluid nanospray. The tagged aldehydes showed signal intensity loss as a result of adding the enhancers to the modifier in the flow injection nSF-MS system. This may be due to the ionization of ammonium clustering with methanol and other alkali metal ions. The decrease in the acidity with added water compared to 0.1 % formic may also have diminished the analyte signal. <sup>57, 58</sup> The observation is more pronounced in 75  $\mu m$  i.d. whereas the modifier effect decreases as the nESI emitter i.d. decrease. <sup>53</sup>

Interfacing SFC-MS faces major challenges of solvent depressurization, phase separation inside the connector, analyte precipitation, and hence reduced MS response. 26 To overcome phase separation, heating the interface connector or adding a make-up flow to the SFC outlet has been performed.<sup>25, 59</sup> Nanospray, make-up flow SF-ESI-MS, and direct SF-ESI-MS were compared to the nSF-MS. Figure 7 shows the difference in signal response using the conventional SF makeup flow to nSF injecting the same 1 µL sample. The comparison showed enhancement of the signal intensity of 2.72E4±0.6 for the 25 μm i.d, 1.54E5±0.2 for the 50 μm i.d, and 2.33E5±0.5 for the 75 μm i.d. on average for the tagged aldehydes. The benefit of nSF-MS is more pronounced as the nESI emitter i.d. increased. The make-up flow resulted in sample dilution and loss of the analytes signal. 25, 60 The predominance of organic media results in formation of methanol adducts as a background interference (Supplemental Figure 7).61 Ionic suppression and the modifier adduct formation may have resulted from injecting more liquid organic makeup.<sup>53</sup> Nanospraying the SF using a split flow system have shown more sensitive detection compared to makeup flow. This may be due to the improved ionization efficiency. 60, 62

To evaluate a direct SF-ESI-MS system, injection of 1 μL sample using a HESI heated source and ZDV connections was evaluated. To achieve stable spray under these conditions, >1 mL/min was needed. Such high flow rates can contaminate the tube lens and skimmer. Splitless flow showed signal intensity drop by 1 order of magnitude compared to makeup flow SF and 2 orders of magnitude compared to the nSF system. The post-BPR split-flow nSF system using a heated interface to maintain the SF state allowed for higher sensitivity without sample dilution. Contrasting the MS response towards the adopted coupling strategies showed a signal intensity gain using the developed split flow system. The nSF-MS signal was 6 times the makeup flow signal and 12 times the direct injection signal. The data indicate that sCO2 as a nanospray carrier fluid exhibits high efficiency ionization. It provided higher signal intensity compared to the SF makeup and splitless flow in an open tube SF emitter system.

#### Conclusion.

Post-BPR split-flow nanospray nSF-MS coupling strategy was developed and evaluated using a fabricated photopolymerized frit embedded in laser pulled capillaries. The heated nanospray emitters (25, 50, and 75  $\mu m$  i.d.) showed improved MS signal response compared to makeup flow SF. The post-BPR split-flow with nano emitters result in smaller electrospray droplets. The sCO2 evaporative properties result in nanospraying smaller initial droplets which eased desolvation, produced higher ionization efficiency, and resulted in enhanced MS response. While not fully investigated in this work, we hypothesize that the supercritical fluid state which is generated before the BPR is maintained until the point of exit from the emitter tip.

This system demonstrates mass sensitive detector response indicating high efficiency electrospray. The size of the emitted droplet is often reported based on conventionally accepted models.<sup>4, 63-65</sup> These models differ in their use of surface tension, either in the numerator or denominator. Because SFs have no surface tension <sup>66</sup>, the models do not hold for nSF-MS. Using these models, the

droplet size from our system would be either zero or infinity, neither of which is physically feasible. Further work is needed to evaluate the electrospray process in nSF systems. It has not escaped our attention that longer alkyl chains levied higher signal responses at equal concentrations. This is possibly due to variations in solvation or mass-discrimination effects. The columbic repulsion increases in the evaporating droplet as the m/z increase.<sup>37</sup>

This work used quaternary amines to investigate desolvation. Future work on proton transfer and analyte hydrophobicity is necessary to characterize the effects of ionization beyond the desolvation discussed here. This will also be used to validate the application of the developed ionization technique in omics analysis of biological samples of diverse chemical compositions and functionalities.

## ASSOCIATED CONTENT

## **Supporting Information**

The Supporting Information is available free of charge on the ACS Publications website.

Myoglobin MS spectrum, pumps pressure changes as a function of methanol percentage change, 3D signal intensity of the tagged aldehydes as a function of pressure and volumetric flow rate using 25, 50, and 75  $\mu m$  i.d. nESI interface, Percentage relative abundance as a function of injected volume, signal suppression effect (PDF link).

#### **AUTHOR INFORMATION**

#### **Corresponding Author**

\* James L. Edwards - Department of Chemistry and Biochemistry, Saint Louis University, 3501 Laclede Ave, St Louis, MO 63103, USA. <a href="http://orcid.org/0000-0003-1063-7518">http://orcid.org/0000-0003-1063-7518</a>, Email: jim.edwards@slu.edu

## Authors

Mahmoud Elhusseiny Mostafa - Department of Chemistry and Biochemistry, Saint Louis University, 3501 Laclede Ave, St Louis, MO 63103, USA. <a href="https://orcid.org/0000-0001-7688-1789">https://orcid.org/0000-0001-7688-1789</a>

James P. Grinias - Department of Chemistry and Biochemistry, Rowan University, 201 Mullica Hill Rd., Glassboro, NJ 08028, USA. https://orcid.org/0000-0001-9872-9630

## **Author Contributions**

**Mahmoud Elhusseiny Mostafa:** Methodology, Data curation, Formal analysis, Writing –review & editing. **James L. Edwards:** Conceptualization, Funding acquisition, Supervision, Writing –review & editing. **James P. Grinias:** Funding acquisition, Writing – review & editing.

#### Notes

The authors declare no competing financial interests.

# ACKNOWLEDGMENT

This work was supported by funding from the Chemical Measurement and Imaging Program in the National Science Foundation Division of Chemistry to J.L.E. (CHE-1904919), and to J.P.G. (CHE-1904454).

#### REFERENCES

1. Edwards, J. L.; Edwards, R. L.; Reid, K. R.; Kennedy, R. T., Effect of decreasing column inner diameter and use of off-line

- two-dimensional chromatography on metabolite detection in complex mixtures. J. Chrom. A 2007, 1172 (2), 127-134.
- 2. El-Faramawy, A.; Siu, K. W. M.; Thomson, B. A., Efficiency of nano-electrospray ionization. J. Am. Soc. Mass. Spectrom. 2005, 16 (10), 1702-1707.
- 3. Konermann, L.; Ahadi, E.; Rodriguez, A. D.; Vahidi, S., Unraveling the Mechanism of Electrospray Ionization. Analytical Chemistry 2013, 85 (1), 2-9.
- 4. Wilm, M. S.; Mann, M., Electrospray and Taylor-Cone theory, Dole's beam of macromolecules at last? International Journal of Mass Spectrometry and Ion Processes 1994, 136 (2), 167-180.
- 5. Cox, J. T.; Marginean, I.; Smith, R. D.; Tang, K., On the ionization and ion transmission efficiencies of different ESI-MS interfaces. J. Am. Soc. Mass. Spectrom. 2015, 26 (1), 55-62.
- 6. Page, J. S.; Kelly, R. T.; Tang, K.; Smith, R. D., Ionization and transmission efficiency in an electrospray ionization—mass spectrometry interface. J. Am. Soc. Mass. Spectrom. 2007, 18 (9), 1582-1590.
- 7. Taylor, L. T., Supercritical fluid chromatography for the 21st century. The Journal of Supercritical Fluids 2009, 47 (3), 566-573.
- 8. Klesper, K., High pressure gas chromatog raphy above critical temperatures. J. Org. Cher 1962, 27, 700-701.
- 9. Zhao, Y.; Woo, G.; Thomas, S.; Semin, D.; Sandra, P., Rapid method development for chiral separation in drug discovery using sample pooling and supercritical fluid chromatography—mass spectrometry. J. Chromatogr. A 2003, 1003 (1), 157-166.
- 10. Wolrab, D.; Frühauf, P.; Gerner, C., Direct coupling of supercritical fluid chromatography with tandem mass spectrometry for the analysis of amino acids and related compounds: Comparing electrospray ionization and atmospheric pressure chemical ionization. Anal. Chim. Acta 2017, 981, 106-115.
- 11. Gazárková, T.; Plachká, K.; Svec, F.; Nováková, L., Current state of supercritical fluid chromatography-mass spectrometry. TrAC, Trends Anal. Chem. 2022, 149, 116544.
- 12. Smith, R. D.; Udseth, H. R., Mass spectrometry with direct supercritical fluid injection. Anal. Chem. 1983, 55 (14), 2266-2272.
- 13. Desfontaine, V.; Veuthey, J. L.; Guillarme, D., Chapter 8 Hyphenated Detectors: Mass Spectrometry. In Supercritical Fluid Chromatography, Poole, C. F., Ed. Elsevier: 2017; pp 213-244.
- 14. Grand-Guillaume Perrenoud, A.; Veuthey, J.-L.; Guillarme, D., Coupling state-of-the-art supercritical fluid chromatography and mass spectrometry: From hyphenation interface optimization to high-sensitivity analysis of pharmaceutical compounds. J. Chrom. A 2014, 1339, 174-184.
- 15. Olesik, S. V., Physicochemical properties of enhanced-fluidity liquid solvents. J. Chromatogr. A 2004, 1037 (1), 405-410.
- 16. Bennett, R.; Olesik, S. V., Enhanced fluidity liquid chromatography of inulin fructans using ternary solvent strength and selectivity gradients. Anal. Chim. Acta 2018, 999, 161-168.
- 17. Beres, M. J.; Olesik, S. V., Enhanced-fluidity liquid chromatography using mixed-mode hydrophilic interaction liquid chromatography/strong cation-exchange retention mechanisms. Journal of Separation Science 2015, 38 (18), 3119-3129.
- 18. Treadway, J. W.; Philibert, G. S.; Olesik, S. V., Enhanced fluidity liquid chromatography for hydrophilic interaction separation of nucleosides. J. Chrom. A 2011, 1218 (35), 5897-5902.
- 19. West, C., Current trends in supercritical fluid chromatography. Analytical and Bioanalytical Chemistry 2018, 410 (25), 6441-6457.
- 20. Li, F.; Hsieh, Y., Supercritical fluid chromatography-mass spectrometry for chemical analysis. Journal of Separation Science 2008, 31 (8), 1231-1237.
- 21. Desfontaine, V.; Guillarme, D.; Francotte, E.; Nováková, L., Supercritical fluid chromatography in pharmaceutical analysis. Journal of Pharmaceutical and Biomedical Analysis 2015, 113, 56-71.
- 22. Miller, L., Preparative enantioseparations using supercritical fluid chromatography. J. Chrom. A 2012, 1250, 250-255.
- 23. Baker, T. R.; Pinkston, J. D., Development and Application of Packed-Column Supercritical Fluid Chromatography/Pneumatically Assisted Electrospray Mass Spectrometry. J. Am. Soc. Mass. Spectrom. 1998, 9 (5), 498-509.

- 24. Hondo, T.; Ota, C.; Miyake, Y.; Furutani, H.; Toyoda, M., Analysis of Nonvolatile Molecules in Supercritical Carbon Dioxide Using Proton-Transfer-Reaction Ionization Time-of-Flight Mass Spectrometry. Analytical Chemistry 2021, 93 (17), 6589-6593.
- 25. Akbal, L.; Hopfgartner, G., Hyphenation of packed column supercritical fluid chromatography with mass spectrometry: where are we and what are the remaining challenges? Analytical and Bioanalytical Chemistry 2020, 412 (25), 6667-6677.
- 26. Tarafder, A., Designs and methods for interfacing SFC with MS. J. Chrom. B 2018, 1091, 1-13.
- 27. Tarafder, A.; Guiochon, G., Extended zones of operations in supercritical fluid chromatography. J. Chrom. A 2012, 1265, 165-175
- 28. Landry, E. S.; Mikkilineni, S.; Paharia, M.; McGaughey, A. J. H., Droplet evaporation: A molecular dynamics investigation. J. Appl. Phys. 2007, 102 (12), 124301.
- 29. Smith, R. D.; Felix, W.; Fjeldsted, J. C.; Lee, M. L., Capillary column supercritical fluid chromatography mass spectrometry. Analytical Chemistry 1982, 54 (11), 1883-1885.
- 30. Nováková, L.; Grand-Guillaume Perrenoud, A.; Francois, I.; West, C.; Lesellier, E.; Guillarme, D., Modern analytical supercritical fluid chromatography using columns packed with sub-2µm particles: A tutorial. Anal. Chim. Acta 2014, 824, 18-35.
- 31. Tarafder, A., Metamorphosis of supercritical fluid chromatography to SFC: An Overview. TrAC Trends in Analytical Chemistry 2016, 81, 3-10.
- 32. Guillarme, D.; Desfontaine, V.; Heinisch, S.; Veuthey, J.-L., What are the current solutions for interfacing supercritical fluid chromatography and mass spectrometry? J. Chrom. B 2018, 1083, 160-170.
- 33. Armbruster, M.; Grady, S.; Agongo, J.; Arnatt, C. K.; Edwards, J. L., Neutron encoded derivatization of endothelial cell lysates for quantitation of aldehyde metabolites using nESI-LC-HRMS. Anal. Chim. Acta 2022, 1190, 339260.
- 34. Haskins, W. E.; Wang, Z.; Watson, C. J.; Rostand, R. R.; Witowski, S. R.; Powell, D. H.; Kennedy, R. T., Capillary LC–MS2 at the Attomole Level for Monitoring and Discovering Endogenous Peptides in Microdialysis Samples Collected in Vivo. Analytical Chemistry 2001, 73 (21), 5005-5014.
- 35. Huang, T.; Armbruster, M. R.; Coulton, J. B.; Edwards, J. L., Chemical Tagging in Mass Spectrometry for Systems Biology. Analytical Chemistry 2019, 91 (1), 109-125.
- 36. Racine, J. S., RSTUDIO: A PLATFORM-INDEPENDENT IDE FOR R AND SWEAVE. Journal of Applied Econometrics 2012, 27 (1), 167-172.
- 37. Olumee, Z.; Callahan, J. H.; Vertes, A., Droplet Dynamics Changes in Electrostatic Sprays of Methanol–Water Mixtures. The Journal of Physical Chemistry A 1998, 102 (46), 9154-9160.
- 38. Werling, J. O.; Debenedetti, P. G., Numerical modeling of mass transfer in the supercritical antisolvent process. The Journal of Supercritical Fluids 1999, 16 (2), 167-181.
- 39. Fujito, Y.; Hayakawa, Y.; Izumi, Y.; Bamba, T., Importance of optimizing chromatographic conditions and mass spectrometric parameters for supercritical fluid chromatography/mass spectrometry. J. Chrom. A 2017, 1508, 138-147.
- 40. Loudon, C.; McCulloh, K., Application of the Hagen—Poiseuille equation to fluid feeding through short tubes. Annals of the Entomological Society of America 1999, 92 (1), 153-158.
- 41. Smith, R. D.; Fjeldsted, J. C.; Lee, M. L., Direct fluid injection interface for capillary supercritical fluid chromatography-mass spectrometry. J. Chromatogr. A 1982, 247 (2), 231-243.
- 42. Glenne, E.; Leśko, M.; Samuelsson, J.; Fornstedt, T., Impact of Methanol Adsorption on the Robustness of Analytical Supercritical Fluid Chromatography in Transfer from SFC to UHPSFC. Anal. Chem. 2020, 92 (23), 15429-15436.
- 43. Cech, N. B.; Enke, C. G., Practical implications of some recent studies in electrospray ionization fundamentals. Mass Spectrometry Reviews 2001, 20 (6), 362-387.
- 44. Amad, M. a. H.; Cech, N. B.; Jackson, G. S.; Enke, C. G., Importance of gas-phase proton affinities in determining the electrospray ionization response for analytes and solvents. Journal of Mass Spectrometry 2000, 35 (7), 784-789.

- 45. Reighard, T. S.; Lee, S. T.; Olesik, S. V., Determination of methanol/CO2 and acetonitrile/CO2 vapor-liquid phase equilibria using a variable-volume view cell. Fluid Phase Equilibria 1996, 123 (1), 215-230.
- 46. Calixte, E. I.; Liyanage, O. T.; Kim, H. J.; Ziperman, E. D.; Pearson, A. J.; Gallagher, E. S., Release of Carbohydrate—Metal Adducts from Electrospray Droplets: Insight into Glycan Ionization by Electrospray. The Journal of Physical Chemistry B 2020, 124 (3), 479-486.
- 47. Calixte, E. I.; Liyanage, O. T.; Gass, D. T.; Gallagher, E. S., Formation of Carbohydrate–Metal Adducts from Solvent Mixtures during Electrospray: A Molecular Dynamics and ESI-MS Study. J. Am. Soc. Mass. Spectrom. 2021, 32 (12), 2738-2745.
- 48. Page, S. H.; Goates, S. R.; Lee, M. L., Methanol/CO2 phase behavior in supercritical fluid chromatography and extraction. The Journal of Supercritical Fluids 1991, 4 (2), 109-117.
- 49. Berger, T. A., Effect of density on kinetic performance in supercritical fluid chromatography with methanol modified carbon dioxide. J. Chrom. A 2018, 1564, 188-198.
- 50. Berger, T. A., Characterization of a 2.6µm Kinetex porous shell hydrophilic interaction liquid chromatography column in supercritical fluid chromatography with a comparison to 3µm totally porous silica. J. Chrom. A 2011, 1218 (28), 4559-4568.
- 51. Tarafder, A.; Kaczmarski, K.; Poe, D. P.; Guiochon, G., Use of the isopycnic plots in designing operations of supercritical fluid chromatography. V. Pressure and density drops using mixtures of carbon dioxide and methanol as the mobile phase. J. Chrom. A 2012, 1258, 136-151.
- 52. Berger, T. A., Quantification of mass flow effects in capillary SFC. Journal of High Resolution Chromatography 1989, 12 (2), 96-100.
- 53. Mostafa, M. E.; Grinias, J. P.; Edwards, J. L., Evaluation of Nanospray Capillary LC-MS Performance for Metabolomic Analysis in Complex Biological Matrices. J. Chrom. A 2022, 462952.
- 54. Urban, P. L., Clarifying Misconceptions about Mass and Concentration Sensitivity. Journal of Chemical Education 2016, 93 (6), 984-987.
- 55. Roy, D.; Wahab, M. F.; Berger, T. A.; Armstrong, D. W., Ramifications and Insights on the Role of Water in Chiral Sub/Supercritical Fluid Chromatography. Analytical Chemistry 2019, 91 (22), 14672-14680.
- 56. Haglind, A.; Hedeland, M.; Arvidsson, T.; Pettersson, C. E., Major signal suppression from metal ion clusters in SFC/ESI-MS Cause and effects. J. Chrom. B 2018, 1084, 96-105.
- 57. Berger, T. A.; Deye, J. F., Role of additives in packed column supercritical fluid chromatography: suppression of solute ionization. J. Chrom. A 1991, 547, 377-392.
- 58. Sindelar, M.; Patti, G. J., Chemical Discovery in the Era of Metabolomics. Journal of the American Chemical Society 2020, 142 (20), 9097-9105.
- 59. Akbal, L.; Hopfgartner, G., Effects of liquid post-column addition in electrospray ionization performance in supercritical fluid chromatography—mass spectrometry. J. Chrom. A 2017, 1517, 176-184.
- 60. Van De Steene, J. C.; Mortier, K. A.; Lambert, W. E., Tackling matrix effects during development of a liquid chromatographic–electrospray ionisation tandem mass spectrometric analysis of nine basic pharmaceuticals in aqueous environmental samples. J. Chrom. A 2006, 1123 (1), 71-81.
- 61. Keller, B. O.; Sui, J.; Young, A. B.; Whittal, R. M., Interferences and contaminants encountered in modern mass spectrometry. Anal. Chim. Acta 2008, 627 (1), 71-81.
- 62. Chetwynd, A. J.; David, A., A review of nanoscale LC-ESI for metabolomics and its potential to enhance the metabolome coverage. Talanta 2018, 182, 380-390.
- 63. Schmidt, A.; Karas, M.; Dülcks, T., Effect of different solution flow rates on analyte ion signals in nano-ESI MS, or: when does ESI turn into nano-ESI? J. Am. Soc. Mass. Spectrom. 2003, 14 (5), 492-500.
- 64. Fernández de la Mora, J.; Loscertales, I., The current transmitted through an electrified conical meniscus. J. Fluid Mech. 1994, 260, 155-184.

Pfeifer, R. J.; Hendricks, C. D., Parametric studies of electrohydrodynamic spraying. AIAA Journal 1968, 6 (3), 496-502.
Reverchon, E.; Cardea, S., Supercritical fluids in 3-D tissue engineering. The Journal of Supercritical Fluids 2012, 69, 97-107.